Inorg. Chem. **2003**, *42*, 5442–5447

The Thermostability and Reactivity of GaP Nanocrystals in Oxygen: From GaP Nanocrystals to Ga_2O_3 Nanocrystals

Shanmin Gao, Yi Xie,* Liying Zhu, and Xiaobo Tian

Structure Research Laboratory, Department of Chemistry, University of Science and Technology of China, Hefei, Anhui 230026, P. R. China

Received March 27, 2003

The thermostability and reactivity of GaP nanocrystals in O_2 were investigated using the thermogravimetric analysis (TGA), differential thermal analysis (DTA), powder X-ray diffraction (XRD), and X-ray photoelectron spectroscopy (XPS) analysis techniques. α-Ga_2O_3 nanoparticles, nano-hollow-particles, or nanorods and nanotubes can be separately obtained from the oxidation of nanocrystalline GaP at 400 °C for 30 min in dry O_2 atmosphere via manipulating different heating rates. Transmission electron microscopy (TEM) and energy-dispersive X-ray spectrometry (EDX) analysis showed that the products were all α-Ga_2O_3 but with different morphologies when different heating rates were applied. The formation mechanisms of the different morphological α-Ga_2O_3 nanocrystals were discussed.

Introduction

Semiconductor nanoparticles are interesting materials because they have chemical and physical properties different from those of the corresponding bulk and isolated atoms or molecules.[1−4] Residing in the mesoscopic regime between the molecular and bulk regimes, semiconductor nanoparticles have unique electronic, magnetic, and optical properties due to their small size and large surface-to-volume (*S*/*V*) ratio.[5,6] During the past decade, the design of novel nanostructured semiconductor materials become a part of frontier research because their properties have potential applications in various fields, such as microelectronics, photocatalysis, nonlinear optics, photoelectrochemistry, imaging science, and electrooptics.[7,8] Among the semiconductor materials, the II−VI group semiconductor nanomaterials have been most widely and deliberately studied, and much work has been done especially on the aspect of preparation techniques and their properties.[9−12] In contrast, the study of the III−V group semiconductor nanomaterials is relatively less, owing to the great difficulty in their preparation.[4] In addition, quantum size effects on the optical properties have been predicted to be more pronounced in the III−V group semiconductor nanomaterials than that in II−VI semiconductor nanomaterials since III−V semiconductor nanomaterials have a greater degree of covalent bonding, a less ionic lattice, and larger exciton diameters.[13] Hence, it is very important to further study the synthesis and properties of III−V semiconductors nanomaterials under mild conditions. Moreover, the application of semiconductors depends on the change of the environment conditions, so studying the influence of environment conditions on the properties of semiconductor nanomaterials is also impending.

GaP is an indirect gap semiconductor and has many important applications in microelectronic devices. However, despite a few reports about the synthesis and properties of GaP nanocrystals,[14−16] very little is known about the thermal stability of III−V semiconductor nanocrystals. In the past

* To whom correspondence should be addressed. E-mail: yxielab@ustc.edu.cn.

(1) Alivisatos, A. P. *Science* **1996**, *271*, 933.
(2) Kamat, P. V. *Prog. Inorg. Chem.* **1997**, *44*, 273.
(3) Collier, C.; Vossmeyer, T.; Heath, J. *Annu. Rev. Phys. Chem.* **1998**, *49*, 371.
(4) Heath, J. R.; Shiang, J. J. *Chem. Soc. Rev.* **1998**, *27*, 65.
(5) Zhang, J. Z. *Acc. Chem. Res.* **1997**, *30*, 423.
(6) Alivisatos, A. P. *J. Phys. Chem.* **1996**, *100*, 13226.
(7) Stafford, U.; Gray, K. A.; Kamat, P. V. *Heterog. Chem. Rev.* **1996**, *3*, 77.
(8) Carter, S. A.; Scott, J. C.; Brook, P. J. *Appl. Phys. Lett.* **1997**, *71*, 1145.
(9) Peng, X.; Schlamp, M. C.; Kadavanich, A. V.; Alivisatos, A. P. *J. Am. Chem. Soc.* **1997**, *119*, 7019.
(10) Alivisatos, A. P.; Barbara, P. F.; Castleman, A. W.; Chang, J.; Dixon, D. A.; Klein, M. L.; McLendon, G. L.; Miller, J. S.; Ratner, M. A.; Rossky, P. J.; Stupp, S. I.; Thompson, M. E. *Adv. Mater.* **1998**, *10*, 1297.
(11) Rogach, A. L.; Kershaw, S. V.; Burt, M. G.; Harrison, M. T.; Kornowski, A.; Eychmüller, A.; Weller, H. *Adv. Mater.* **1999**, *11*, 552.
(12) Anderson, M. A.; Gorer, S.; Penner, M. R. *J. Phys. Chem. B* **1997**, *101*, 5895.
(13) Brus, L. E. *J. Phys. Chem.* **1983**, *79*, 5566.

10.1021/ic034327n CCC: $25.00
Published on Web 07/30/2003

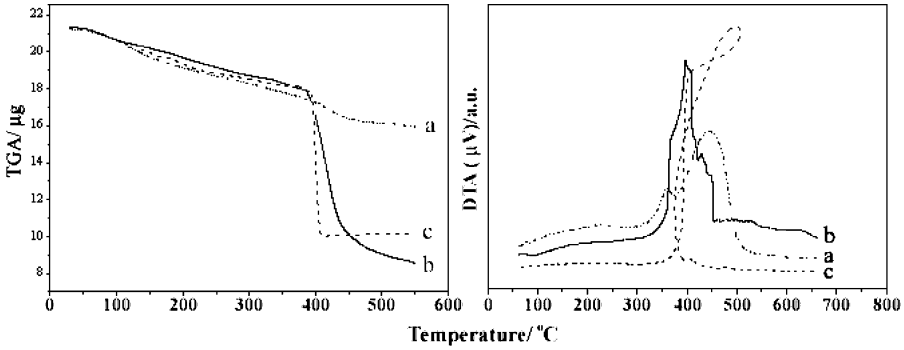

Figure 1. Thermogravimetric analyses and differential thermal analysis of GaP nanocrystals in O_2 flow at different heating rates from 30 to 550 °C. The heating rates are (a) 5 °C/min; (b) 10 °C/min, and (c) 20 °C/min.

several years, our group has been devoted to the synthesis and properties of GaP nanocrystals, and many significant results have been found,[17−21] which provide an important and reliable basis for application of GaP nanocrystals in practice. In this paper, the thermal stability and reactivity of GaP nanocrystals in O_2 atmosphere were studied in detail, and some new phenomena arose. The results showed that GaP nanocrystals were oxidized at lower temperature than bulk GaP material and different morphologies of α-Ga_2O_3 were obtained by controlling the heating rates. This result provides a convenient path for producing α-Ga_2O_3 with different morphologies, such as nanoparticles, nano-hollow-particles, nanorods, and nanotubes.

Experimental Section

The starting GaP nanocrystals used in the present study were synthesized in the benzene thermal route using Na_3P and $GaCl_3$ as the raw materials, which has been described elsewhere.[19] The thermostability behavior of GaP nanocrystals in O_2 was thoroughly studied through thermogravimetric analysis (TGA) and differential thermal analysis (DTA) techniques, which were performed using a Perkin-Elmer DC/2C type TG-DTA instrument at different heating rate. The reaction process of GaP nanocrystals in O_2 was carried out in a horizontal quartz tube of a conventional tubular furnace. A 2 g portion of GaP nanocrystals was loaded into a quartz crucible, which was then horizontally placed in a quartz tube of a tubular furnace. First, the quartz tube was evacuated for 20 min by a vacuum pump. After the quartz tube was ventilated by high purity (99.99%) O_2 at a flow of about 20 sccm (standard cubic centimeters per minute) for several minutes, it was heated to 400 °C at different heating rates (5, 10, and 20 °C/min) and kept constant for different times. A unit mass flow controller controlled the flow velocity of O_2 gas. Gray-white or white products were cooled to room temperature and sealed into glass tubes for further characterization.

The phases of the products are detected at a scanning rate of $0.02°\cdot s^{-1}$ in the 2θ range from 20° to 60° using a D/max-γA model X-ray diffractometer with Ni-filtered Cu Kα radiation while the starting GaP nanoparticles were recorded at a scanning rate of $0.05°\cdot s^{-1}$. X-ray photoelectron spectroscopy (XPS) was performed on a VGESCALAB 220i-XL X-ray photo spectrometer with Al Kα (1186.6 eV) radiation as the exciting source; measurements were performed at pressures lower than 1×10^{-8} Torr. The binding energies obtained in the XPS analysis were corrected by referencing the C 1s peak to 284.60 eV. A Fourier transform infrared spectrometer (FT-IR) spectrum of pellets of the samples mixed with KBr was recorded on a Nicolet Magna-IR 750 FTIR spectrometer at a resolution of 4 cm^{-1}. Transmission electron microscopy (TEM) images of the samples were obtained from a Hitachi model H800 transmission electron microscope using an accelerating voltage of 200 kV. Samples for experiments for TEM investigations were briefly ultrasonicated in ethanol, and then, a drop of the suspension was placed on a holey copper grid with carbon film.

Results and Discussion

A detailed thermostability behavior of the GaP nanocrystals was studied via thermogravimetric analysis (TGA) and differential thermal analysis (DTA), which were collected under O_2 flow with 5, 10, and 20 °C /min heating rates, respectively. The typical TGA-DTA profiles are shown in Figure 1.

From the TGA and DTA results, one can see that some changes have occurred and obviously chemical reactions of GaP nanocrystals in O_2 take place. These interesting phenomena give us inspiration about thoroughly studying the reactivity of GaP nanocrystals in O_2, and detailed reaction processes of GaP nanocrystals in O_2 have described in the Experimental Section. After heat treatment in O_2 at different temperatures or times, it was found that the gray powders of GaP nanocrystals turned into gray-white or white powders. These changes will be explained in a later section.

XRD was used to examine the crystal structure and phase purity of the products, and the typical XRD patterns of the resulting materials are shown in Figure 2. α-Ga_2O_3 is obtained from GaP nanocrystals at the heating rate of 5 °C/min, and the corresponding XRD pattern is shown in Figure 2b. All the reflection peaks are indexed to those of α-Ga_2O_3 (JCPDS file 6-503), which is the low-temperature polymorph phase of the gallium oxides. Figure 2c displays the XRD pattern of the products prepared from the heat treatment of GaP nanocrystals in O_2 at 400 °C for 30 min at the heating

(14) Jouet, R. J.; Wells, R. L.; Rheingold, A. L.; Incarvito, C. D. *J. Organomet. Chem.* **2000**, *601*, 191.
(15) Kher, S. S.; Wells, R. L. *Chem. Mater.* **1994**, *6*, 2056.
(16) Micic, O. I.; Sprague, J. R.; Curtis, C. J.; Jones, K. M.; Machol, J. L.; Nozik, A. J.; Giessen, H.; Fluegel, B.; Mohs, G.; Peyghambarian, N. *J. Phys. Chem.* **1995**, *99*, 7754.
(17) Gao, S. M.; Cui, D. L.; Huang, B. B.; Jiang, M. H. *J. Cryst. Growth* **1998**, *192*, 89.
(18) Cui, D. L.; Gao, S. M.; Huang, B. B.; Yu, S. Q.; Qin, X. Y.; Jiang, M. H. *Chin. Phys. Lett.* **1998**, *15*, 307.
(19) Gao, S. M.; Xie, Y.; Lu, J.; Du, G. A.; He, W.; Cui, D. L.; Huang, B. B.; Jiang, M. H. *Inorg. Chem.* **2002**, *41*, 1850.
(20) Gao, S. M.; Lu, J.; Zhao, Y.; Chen, N.; Xie, Y. *Chem. Commun.* **2002**, 2880.
(21) Gao, S. M.; Lu, J.; Chen, N.; Zhao, Y.; Xie, Y. *Chem. Commun.* **2002**, 3064.

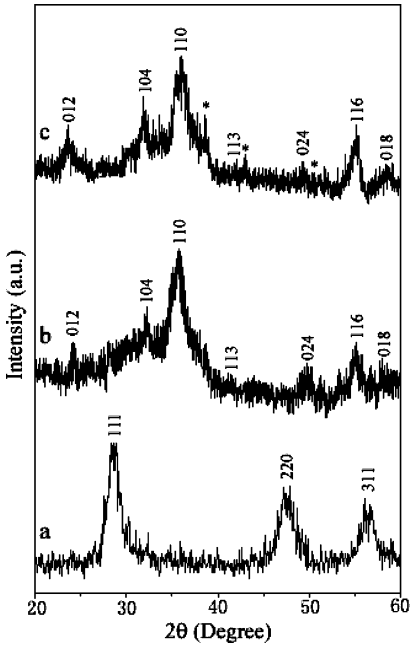

Figure 2. XRD patterns of (a) the starting GaP nanocrystals, (b) the sample obtained from the heat treatment of GaP nanocrystals at 400 °C for 30 min at a heating rate of 5 °C/min, and (c) the unwashed samples obtained from the heat treatment of GaP nanocrystals at 400 °C for 30 min at a heating rate of 10 or 20 °C/min. Asterisk indicates the residual elemental Ga.

rate of 10 °C/min or 20 °C/min, indicating the products are the α-Ga_2O_3 with the coexistence of minor elemental Ga (denoted with an asterisk in Figure 2c, JCPDS file 31-0539). The minor elemental Ga can be easily removed by treatment using 1 N hydrochloric acid, and then, α-Ga_2O_3 can be obtained, which is confirmed by an XRD pattern similar to that in Figure 2b. The XRD patterns of all the products are quite different from that of the starting GaP nanoparticles (as shown in Figure 2a). The results show that α-Ga_2O_3 formed in the heat treatment of GaP nanocrystals in O_2 via a P−O metathesis reaction; namely, P atoms escape from the GaP nanocrystals while Ga atoms combined with O atoms.

The morphology and structure of the products obtained from the heat treatment of GaP nanocrystals in O_2 at different heating rates have been further characterized by TEM. Figure 3a shows the TEM image of starting GaP nanocrystals with diameter in the range 9 ± 2 nm. Figure 3b shows that the α-Ga_2O_3 obtained from the heat treatment of GaP nanocrystals in O_2 at 400 °C for 30 min at the heating rate of 5 °C/min consists of uniform spherical nanoparticles with the diameter of 45 ± 5 nm, which is in good agreement with the XRD result calculated by Scherrer equation. They exhibit the similar morphology with the starting GaP nanocrystallites, and the only difference is that the resulting Ga_2O_3 nanocrystals are larger than the starting GaP nanocrystals due to the heating treatment at 400 °C. But for the α-Ga_2O_3 fabricated at 400 °C for 30 min at heating rates of 10 and 20 °C/min, the morphologies of the products are quite different from the product obtained at 400 °C for 30 min at a heating rate of 5 °C/min. As shown in Figure 3c,d, the product is nano-hollow-particles with the diameter 18−22 nm and the hollow pore about 8−10 nm at the heating rate

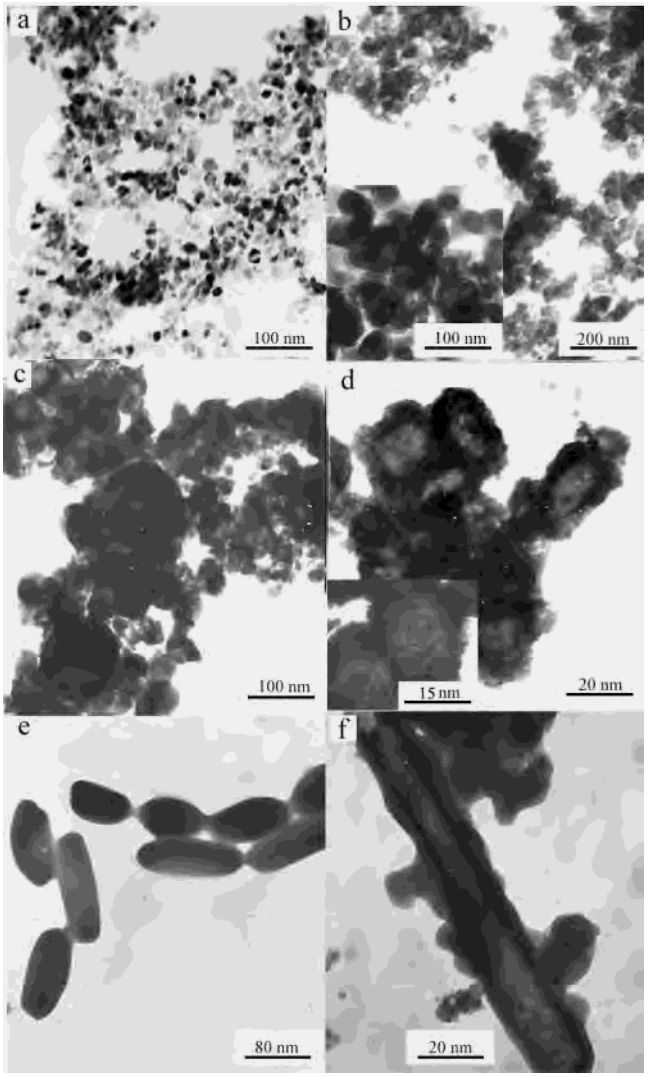

Figure 3. TEM images of (a) the starting GaP nanocrystals, (b) α-Ga_2O_3 nanoparticles obtained from heat treatment of GaP nanocrystals in O_2 at 400 °C for 30 min at a heating rate of 5 °C/min (the inset is the high-magnification image), (c) α-Ga_2O_3 hollow particles obtained from heat treatment of GaP nanocrystals in O_2 at 400 °C for 30 min at a heating rate of 10 °C/min, (d) the high-magnification image for part c, (the inset is the higher-magnification image), and (e) and (f) α-Ga_2O_3 nanorods and nanotubes obtained from heat treatment of GaP nanocrystals in O_2 at 400 °C for 30 min at a heating rate of 20 °C/min.

of 10 °C/min. The inset image with higher magnification clearly exhibits its hollow structure. At the heating rate of 20 °C/min, the product is nanorods with the diameters of ca. 30−40 nm and lengths of 80−100 nm (Figure 3e), and some nanotubes were found to coexist with the nanorods, as shown in Figure 3f.

An energy-dispersion X-ray spectroscopy (EDX) measurement attached to the TEM was employed to analyze the chemical composition of Ga_2O_3 over a large area on the samples obtained from the heat treatment of GaP nanocrystals in O_2 at 400 °C at different heating rates. All the EDX spectra (Figure 4) showed gallium, oxygen, and copper peaks. It is obvious that the copper peak is caused by the copper grid used to clamp the nanocrystals. EDX quantitative microanalysis revealed that Ga and O have an approximate composition of Ga_2O_3 with a predominance of oxygen and

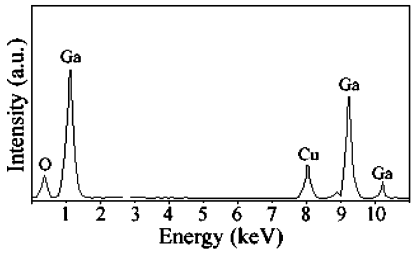

Figure 4. EDX spectrum of the sample obtained from the heat treatment of GaP nanocrystals in O_2 at 400 °C for 30 min at the heating rate of 20 °C/min.

gallium elements with the atomic ratio of O and Ga being ca. 60.7%/39.3%. In addition, X-ray photoelectron spectroscopy (XPS) was used to investigate the elemental composition of the starting GaP nanocrystals and the oxidation products of the nanocrystals. The binding energy values of the Ga_{3d}, P_{2p}, and O_{1s} core levels agree well with such a chemical environment of the GaP and Ga_2O_3. This clearly indicates that the O_2 molecules must be chemically bonded to Ga atoms, presumably forming O−Ga bonds.

These results indicated that, no matter what heating rate was used in our experiments, the O−P metathesis reaction occurred. The replacement of P by O atoms is facilitated by the fact that P is more volatile than Ga and tends to escape from GaP upon thermal annealing. The thermal stability of GaP powder under flowing O_2 reveals that there are some volatile or decomposable components, which has been confirmed by the weight loss on the TGA curves. The first weight loss is laggard in the temperature range 30−350 °C, which is attributed to the elimination of surface capping groups such as the oxide layer and adsorbed water in the starting GaP nanocrystals. Because of the higher surface areas and reactivity of the nanocrystals, the atoms on the surface are much more easily oxidized when they are exposed to air. Similar phenomena of oxidization layer have been reported on InP[22] and InAs[23] nanocrystals. The oxide layer has been detected by the XPS technique, and the adsorbed water can be detected by Fourier transform infrared spectroscopy (FT-IR) (XPS and FT-IR spectrum not shown). With increasing temperature, from the TGA and DTA profiles one can see that the pronounced weight loss step is found in the temperature range 350−500 °C in O_2, which can be ascribed to the loss of phosphorus for GaP nanocrystals and the O−P metathesis reaction. So, we think the feasible temperature of the metathesis reaction of O−P is 400 °C in O_2.

On the basis of the experimental observations, a growth mechanism is proposed, and a schematic representation of the formation α-Ga_2O_3 nanocrystals with different morphologies is given in Figure 5.

As we know, the surface area of nanocrystals is much larger than that of the bulk materials, and there exist a lot of vacancies and dangling bonds on the surface of nanocrystals.

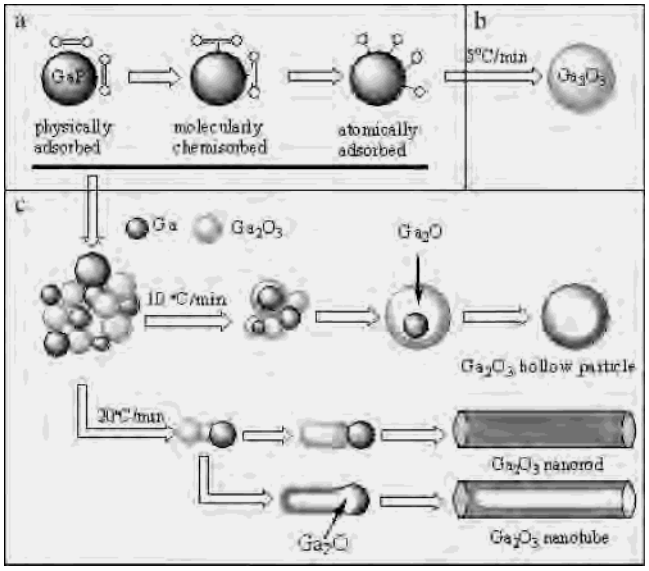

Figure 5. Proposed mechanism of the formation of α-Ga_2O_3 nanocrystals: (a) the surface adsorption reaction of O_2 on GaP nanocrystals and the nucleation of Ga_2O_3, (b) the growth of α-Ga_2O_3 nanoparticles at lower heating rate, and (c) step growth of α-Ga_2O_3 nano-hollow-particles, nanorods, or nanotubes at higher heating rate.

In our experiment, the O_2 molecules are adsorbed onto the surface of the starting GaP nanocrystals during the initial heating stage (Figure 5a). First, the adsorbate (here O_2) forms the adatom on the surface of GaP nanocrystals (adsorbent), and it is physically adsorbed via a van der Waals force. The vacancies and dangling bonds on the surface of GaP nanocrystals supply a favorable environment for O_2 molecules to form bonds. Upon elevating the temperature, chemical bonding of O and Ga formed; that is to say, the molecular chemisorbs occur, producing the local sorbate−sorbent bonding adsorption or activated adsorption. As a result, the O_2 molecules can be activated on the surface of GaP nanocrystals at a rather lower temperature, remarkably weakening the strength of O═O on the surface of GaP nanocrystals in O_2. The activated O atoms form, and a kind of atomic adsorption occurs; then, the metathesis reaction of O and P takes place. It is well-known that the thermal oxidation of compound semiconductors such as GaAs and GaP-based materials is a much more complex phenomenon.[24,25] For bulk GaP materials, the completed oxidation takes place only when the temperature is higher than 800 °C.[26,27] But in our experiments, the metathesis reaction of O and P in nanocrystalline GaP takes place at 400 °C. The remarkable temperature reduction is attributed to the larger surface area of nanocrystals as compared to that of the corresponding bulk materials, and there exist a lot of vacancies and dangling bonds on the surface of nanocrystals. The high surface area and reactivity of nanocrystalline GaP

(22) Guzelian, A. A.; Katari, J. E. B.; Kadavanich, A. V.; Banin, U.; Hamad, K.; Juban, E.; Alivisatos, A. P.; Wolters, R. H.; Arnold, C. C.; Heath, J. R. *J. Phys. Chem.* **1996**, *100*, 7212.
(23) Xie, Y.; Yan, P.; Lu, J.; Wang, W.; Qian Y. *Chem. Mater.* **1999**, *11*, 2619.
(24) Thurmond, C. D.; Schwartz, G. P.; Kammlott, G. W.; Schwartz, B. *J. Electrochem. Soc.* **1980**, *127*, 1366.
(25) Spicer, W. E.; Lindau, I.; Skeath, P.; Su, C. Y. *J. Vac. Sci. Technol.* **1980**, *1019*, 17.
(26) Uekusa, S.; Yano, Y.; Fukaya, K.; Kumagai, M. *Nuclear Instrum. Methods Phys. Res., Section B* **1997**, *127*, 541.
(27) Van Velsen, W. J. M.; Morgan, A. E. *Surf. Sci.* **1973**, *39*, 255.

directly result in the formation of α-Ga_2O_3 at lower temperature, lower pressure, and shorter time.

At a lower heating rate (5 °C/min), the oxidized product is only α-Ga_2O_3 nanoparticles rather than nanorods and hollow particles. Under this condition, the desorption of P, absorption of O, and oxidation is a synchronous process in the GaP nanocrystals, and no excess Ga droplets form. This has been validated by the XRD pattern (as shown in Figure 2b). At the same time, P atoms could be easily oxidized into PO_x gas flowing out of the chamber, which is indeed a smokelike gas observed in our experiment. Thus, α-Ga_2O_3 gradually forms on the surface of the GaP nanoparticles during this process. The total reaction can be described as eq 1.

$$2GaP + ({}^3/_2 + x)O_2 \rightarrow Ga_2O_3 + 2PO_x \quad (1)$$

The resulting α-Ga_2O_3 nanoparticles inherit the GaP morphology, which can explain the similarity of the morphology of the resulting α-Ga_2O_3 and the starting GaP nanoparticles (Figure 5b).

However, when the heating rate is higher (≥10 °C/min), the reaction is complicated, and the initial chemical reaction is the desorption of P from GaP nanocrystals, as described as eq 2.

$$GaP \rightarrow Ga + P \quad (2)$$

The desorption chemical reaction is dominant and rapid. Then, the newborn gallium forms first with such high reactivity as to quickly react with O_2 to produce many α-Ga_2O_3 nuclei (that is eq 3).

$$Ga + O_2 \rightarrow Ga_2O_3 \quad (3)$$

A higher heating rate also promotes the newborn Ga coalescence along with its oxidation, resulting in the appearance of smaller droplets of Ga. The α-Ga_2O_3 nucleus start to aggregate and act as the nucleation seeds; then, step growth goes on, with a Ga droplet being pushed outward by the descending α-Ga_2O_3 (Figure 5c). The formed Ga droplets play a crucial role in the growth of α-Ga_2O_3 nano-hollow-particles or nanorods, which have been confirmed by the XRD of the products obtained at the heating rates of 10 and 20 °C/min, as shown in Figure 2c.

α-Ga_2O_3 nano-hollow-particles were obtained at the heating rate of 10 °C/min, and its growth mechanism can be schematically described in Figure 5c. In this process, the Ga droplets react with O_2 in the outer surface to form α-Ga_2O_3 (eq 3), which lay over the surface of Ga droplets. The renascent α-Ga_2O_3 outer layer reacts with inner Ga droplets in the interface to produce Ga_2O until all Ga droplets were exhausted as described in eq 4.

$$4Ga(l) + Ga_2O_3(s) \rightarrow 3Ga_2O(g) \quad (4)$$

The Ga_2O will automatically get out from the products due to high volatilization,[28,29] resulting in the formation of the final nano-hollow-particle structures, which is in fact indeed an oxidation−evaporation process.

For the α-Ga_2O_3 nanorods and nanotubes obtained at the heating rate of 20 °C/min, it can be understood on the basis of the vapor−liquid−solid (VLS) mechanism, which is widely used to explain the growth of fiberlike semiconductors.[30−32] The main characteristic of this mechanism is the presence of intermediates, which serve as catalysts between the vapor feed and the solid growth at elevated temperatures under chemical vapor deposition conditions. In this work, the intermediate Ga governs the growth of α-Ga_2O_3 nanorods or nanotubes, and Figure 5c schematically depicts the mechanism of the formation of α-Ga_2O_3 nanorods and nanotubes. For the nanorods, the growth is controlled by the crystal growth rate at the liquid−solid interface (kinetically limited). Diffusion of atoms in the droplet is then relatively faster with respect to crystal growth, and the concentration is uniform throughout the droplet. Growth takes place at the entire liquid−solid junction, giving rise to solid rods. As regards to the nanotubes, the growth is the diffusion limited. The growth rate has increased with respect to the rate of diffusion as the concentration of atoms in the droplets has been depleted. At the liquid−solid interface, the nucleation front is ring-shaped, giving rise to the growth of tubes. An analogous growth mechanism was proposed for the growth of hollow and solid carbon nanofibers.[33] In the process of formation of nanorods or nanotubes, reaction 4 should also take place at the interface of Ga and Ga_2O_3.

The described mechanisms showing that α-Ga_2O_3 can form in GaP via the O−P metathesis are directly supported by the thermostability study of GaP nanocrystals in O_2. At a lower heating rate, the desorption of P and oxidation are synchronous processes; accordingly, the weight loss should be laggard. But when at higher heating rate, the desorption of P is preferential, so the weight loss should be precipitous. The typical TGA results in Figure 1 are completely in accord with this conclusion. One can see that, at the heating rate of 5 °C/min (Figure 1a), the weight loss is laggard; i.e., reaction 1 takes place in this process. The O and Ga atoms can be completed miscible by an oxidation process since the O and Ga atoms can form a stable electrovalent bond, resulting in the final formation of Ga_2O_3 nanoparticles. In Figure 1a, if we eliminate the effects of the oxide layer and adsorbed water in the starting GaP nanocrystals, the weight loss is estimated to be 7.1%, according with the value of 6.92% calculated by eq 1. At the heating rate of 10 or 20 °C/min, a precipitous line was obtained (Figure 1b,c), illuminating the weight loss much more quickly than at the heating rate of 5 °C/min, which is also accordance with the proposed mechanism. In both cases, at higher heating rates, reaction 2 becomes preferential and rapid, followed by reaction 3. Then, the

(28) Wu, X. C.; Song, W. H.; Huang, W. D.; Pu, M. H.; Zhao, B.; Sun, Y. P.; Du, J. J. *Chem. Phys. Lett.* **2000**, *328*, 5.
(29) Gautam, G.; Govindaraj, A.; Rao, C. N. R. *Chem. Phys. Lett.* **2002**, *351*, 189.
(30) Huang, M. H.; Wu, Y.; Feick, H.; Tran, N.; Weber, E.; Yang, P. *Adv. Mater.* **2001**, *13*, 113.
(31) Shi, W. S.; Zheng, Y. F.; Wang, N.; Lee, C. S.; Lee, S. T. *Adv. Mater.* **2001**, *13*, 591.
(32) Gudiksen, M. S.; Lieber, C. M. *J. Am. Chem. Soc.* **2000**, *122*, 8801.
(33) Snoeck, J. W.; Froment, G. F.; Fowles, J. *J. Catal.* **1997**, *169*, 240.

resulting Ga atoms react with the renascent Ga_2O_3 to produce Ga_2O via reaction 4, but the Ga_2O is volatile and gets out of the system. So, considering the two weight loss processes, the total weight loss is much greater at the higher heating rates. Further analysis can easily find that the weight loss at the heating rate of 10 °C/min should be more than that at the heating rate of 20 °C/min due to the different mechanism of the formation of nano-hollow-particles and 1D nanostructures. At the heating rate of 10 °C/min, the Ga droplet surface was covered by the renascent Ga_2O_3 layer, and the contact interface of Ga and Ga_2O_3 is large, resulting in a mass of Ga_2O form via reaction 4, so the weight loss is the largest. Meanwhile, at the heating rate of 20 °C/min, the faster growth to 1D nanostructures makes less contact between Ga and Ga_2O_3; thus, fewer volatile Ga_2O species formed and left the system, and the weight loss is relatively less. From Figure 1b,c, the weight loss can be calculated as 51.1% and 43.3% for the heating rate of 10 and 20 °C/min, respectively, which supports the described analysis and the proposed formation mechanism.

Conclusion

In conclusion, GaP nanocrystals are not stable in O_2 at elevated temperature and can easily be oxided at a rather lower temperature of 400 °C, much lower than that of the bulk GaP materials since the large surface area of the starting GaP nanocrystalline can reduce remarkably the difficulty of oxidation. α-Ga_2O_3 with different morphologies, such as nanoparticles, nano-hollow-particles or nanorods and nanotubes can be obtained via manipulating the heating rates at 5, 10, and 20 °C/min, respectively. The thermostability of GaP nanocrystals in O_2 has been in detail explored and supported by the proposed formation mechanism of Ga_2O_3 with different morphologies. This study of the thermostability of GaP nanocrystals in O_2 not only provides an important and reliable basis for application of GaP nanocrystals in practice to the request for environment conditions, but also can be used to synthesize different morphologies of Ga_2O_3 nanocrystals via controlling the heating rates.

Acknowledgment. We gratefully acknowledge financial support from the National Natural Science Foundation of China, Chinese Ministry of Education, and Chinese Academy of Sciences. We thank Dr. Y. W. Ding for his discussion of the TGA results.

IC034327N